

## DAMAGE PROGRESSION IN RUBBLE-MOUND BREAKWATERS SCALE MODEL TESTS UNDER DIFFERENT STORM SEQUENCES

RUTE LEMOS<sup>1</sup>, MARIA GRAÇA NEVES<sup>2</sup>, CONCEIÇÃO JUANA FORTES<sup>3</sup>, ANA MENDONÇA<sup>4</sup>, RUI  
CAPITÃO<sup>5</sup>, MARIA TERESA REIS<sup>6</sup>

*1* Laboratório Nacional de Engenharia Civil, [rlemos@lnec.pt](mailto:rlemos@lnec.pt)

*2* Laboratório Nacional de Engenharia Civil, [gneves@lnec.pt](mailto:gneves@lnec.pt)

*3* Laboratório Nacional de Engenharia Civil, [jfortes@lnec.pt](mailto:jfortes@lnec.pt)

*4* Laboratório Nacional de Engenharia Civil, [amendonca@lnec.pt](mailto:amendonca@lnec.pt)

*5* Laboratório Nacional de Engenharia Civil, [rcapitao@lnec.pt](mailto:rcapitao@lnec.pt)

*6* Laboratório Nacional de Engenharia Civil, [treis@lnec.pt](mailto:treis@lnec.pt)

### ABSTRACT

This paper describes the 2D physical model tests performed for a rock armour breakwater at LNEC's facilities, under the framework of the HYDRALAB+ project. The aim of the present work was to evaluate damage evolution under different approaches of storm sequences, corresponding to different climate change scenarios. The tested wave conditions intended to simulate different sequences of water levels (low water and high water), significant wave heights and peak periods. Damage evaluation was based on the traditional visual method and on stereo-photogrammetric techniques. Results in terms of the non-dimensional damage parameter, the non-dimensional damage depth and the percentage of displaced armour units are compared for the different storm sequences.

**KEYWORDS:** Physical model, Damage evolution, Climate change, Storm sequences

### 1 INTRODUCTION

With the predicted climate change a large number of structures will need upgrading or, in some cases, relocation of facilities and population, in order to reduce risk of damage and loss of life. Understanding damage progression under future climate change scenarios is of utmost importance for effective management of coastal defenses.

Since there is a significant uncertainty in predicting the effects of climate change in the variables driving the design of coastal structures (i.e., establishing the sea level rise or predicting extreme events), the use of scenarios, estimating possible future realities in the medium to long terms, is of paramount importance. This is transferable to the planning and operation of physical model studies: since these are time consuming and expensive, the key question is how to properly select representative conditions to be included in the testing programme. In addition, the relevance of reproducing sequences of extreme events over the structure life span, including cumulative effects, needs to be highlighted. Cumulative effects due to storm sequences could lead to progressive failures, due to, for instance, armour instability and related overtopping of the structures. Therefore, a correct description of storm evolution is deemed fundamental for analysing the damage progression and its impact on wave overtopping, HYDRALAB+ (2017).

The aim of this work is to evaluate, on two-dimensional (2D) physical model tests, the damage evolution of a section of a rubble-mound breakwater, under three different approaches of storm sequences: Approach A) simulates increasing wave heights with increasing peak period and water level; Approach B) simulates a constant wave period, alternating water levels and increasing significant wave height; Finally, Approach C) simulates, for two water levels, a standard storm build-up, with a constant peak period.

In all approaches, irregular wave tests were conducted for water levels and significant wave heights corresponding to extreme events related with climate change scenarios. Measuring equipment was deployed on the flume to evaluate the free-surface elevation in different positions, the wave run-up and the overtopping over the structure.

Concerning damage evaluation, two techniques were used: visual observation and stereo-photogrammetric techniques. With the results of those techniques, it was possible to evaluate the non-dimensional damage parameter ( $S$ ), the non-dimensional eroded depth ( $e/D_{n50}$ ) and the percentage of displaced armour units ( $D$ ). Comparisons between damage parameters for the different storm sequence approaches (associated to the same number of climate change scenarios) allowed the evaluation of its influence on the damage progression of this particular rubble-mound breakwater.

The next sections describe the physical model setup and the main results of the tests, followed by a discussion on the results and the main conclusions of this work.

## 2 MATERIALS AND METHODS

### 2.1 Physical scale model

#### Physical model setup and equipment

LNEC's experiments were performed at the Ports and Maritime Structures Unit (NPE) of the Hydraulics and Environment Department, in a wave flume (COI 1) approximately 50 m long, with an operating width of 80 cm and an operating water depth of 80 cm.

The flume is equipped with a piston-type wave-maker embedding an active wave absorption system, AWASYS (Troch, 2005) for the dynamic absorption of unwanted reflected waves.

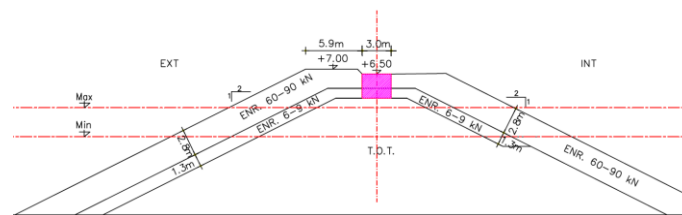


Figure 1. Breakwater cross-section at prototype scale (natural seabed at -8.1 m (CD); CD – chart datum).

The breakwater's cross-section set up at the flume is presented in Figure 1, at a prototype scale. The tested model is a multi-layer rubble-mound breakwater, with a trapezoidal core covered by 2 rock layers, with a porosity of ~ 37% and a 1:2 slope.

The physical model was built and operated according to Froude's similarity law, with a geometrical scale of 1:30, as to ensure reduced scale effects (wave heights should lead to values of the Reynolds number  $Re > 3 \times 10^4$ ).

For that scale, the construction of the physical model began with the application of a foreshore slope of 2%. Then, the breakwater model was built, Figure 2a. The trunk section of the breakwater model was 0.78 m wide. The first two layers of the breakwater were divided into three main parts, and the rocks were painted with different colors. This procedure helped the identification of falls and displacements of rocks during the tests and helped also the photogrammetric surveys. Finally, the experimental equipment was set up - see Figure 2b.

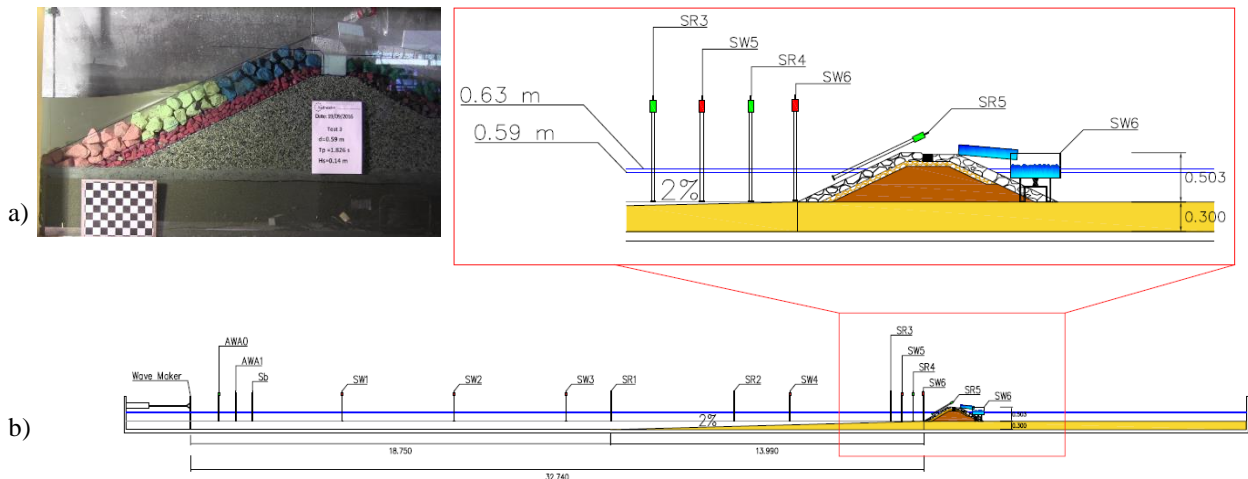


Figure 2. Physical model: a) breakwater cross-section at model scale; b) sketch of the experimental setup in the wave flume.

The flume was equipped with twelve resistive-type wave gauges deployed along its length, to measure the free-surface elevation at different locations, Figure 2b and Figure 3a. In order to measure run-up levels, an additional gauge was placed on the model armour layer slope, Figure 3b.

The equipment used to collect the volume of water that overtopped the structure consisted on a tank, located at the back of the structure. The water was directed to the tank by means of a chute, 40 cm wide, Figure 3c. The overtopping tank was placed over a weighing scale (KERN KXS-TM), which also allowed the measurement of the overtopping volumes, Figure 3c. The measured data were collected as time series and stored, in digital format, at a frequency of 1 Hz.

A pump was positioned inside the tank to remove the overtopping water when the reservoir was almost full.

For damage assessment, two methods were used. The counting of falls and movements of the armour units was performed by visual observation and photo captures of the breakwater cross-section with a standard camera. The stereo-photogrammetry technique used two DSLR cameras (Canon EOS 600D), fitted with fixed focal length lenses (Canon EF 35mm  $f/2$ ), mounted side by side in a frame. This setup enabled both cameras to simultaneously photograph the same scene (Figure 4). All tests were also video-recorded using 2 video cameras, one above the model and the other on the its side, Figure 4. Those cameras were responsible for the run-up and damage measurements.



**Figure 3. Measuring equipment: a) wave gauges to measure free-surface elevation; b) run-up wave gauge; c) chute, overtopping tank, load cell and water-level gauge for measuring overtopping variation.**



**Figure 4. Photographic equipment: a) video cameras; b) photographic cameras**

### Incident wave conditions

The tested wave conditions were meant to simulate storm sequences with no reconstruction between tests. The values of water levels, peak periods and significant wave heights were chosen in order to simulate extreme events related with climate change scenarios, with wave steepnesses between 0.9 and 1.5.

In detail, the test conditions are presented in Table 1, in which  $H_s$  represents the significant wave height at the toe of the structure and  $T_p$  is the corresponding peak period.

Irregular wave tests were carried out, according to a JONSWAP empirical spectrum, with the median peak enhancement factor,  $\gamma = 3.3$ . The test duration was 2400 s for the prototype peak period of 12 s (corresponding to about 1000 waves).

After the initial calibration (Lemos and Santos, 2013; Lemos et al., 2017), the procedure for each test was: 1) Check the water level; 2) Take a pair of photos of the cross-section of the model with the two photogrammetric cameras above it (before starting each test), corresponding to survey  $T0$ ; 3) Generate the incident wave conditions of a test, according to Table 1; 4) Start recording data from all the measuring equipment (wave gauges, load cell, video cameras, etc.). At the end of the test (after 2400 s): 5) Stop recording data by the different measuring equipment and save them; 6) Count the number of unit blocks that fell or moved by visual observation; 7) Take photos with the common camera of the cross-section of the model; 8) Take a pair of photos of the cross-section of the model with the two photogrammetric cameras above it. This corresponds to survey  $T(n)$  (being  $n$  the test number). After the storm sequence, a reconstruction of the model was conducted.

**Table 1. Test conditions at the structure toe**

Storm sequence	Test number	Prototype			Model		
		Water depth (m)	$T_p$ (s)	$H_s$ (m)	Water depth (m)	$T_p$ (s)	$H_s$ (m)
A	1	9.1	10	3.2	0.30	1.826	0.107
	2	9.1	10	3.7	0.30	1.826	0.123
	3	9.1	10	4.2	0.30	1.826	0.140
	4	10.1	11	3.7	0.34	2.008	0.123
	5	10.1	11	4.2	0.34	2.008	0.140
	6	10.1	11	4.7	0.34	2.008	0.157
	7	10.1	11	5.2	0.34	2.008	0.173
<b>Reconstruction</b>							
B	8	11.1	12	3.7	0.37	2.191	0.123
	9	8.1	12	3.7	0.27	2.191	0.123
	10	11.1	12	4.2	0.37	2.191	0.140
	11	8.1	12	4.2	0.27	2.191	0.140
	12	11.1	12	4.7	0.37	2.191	0.157
	13	8.1	12	4.7	0.27	2.191	0.157
	14	11.1	12	5.2	0.37	2.191	0.173
	15	8.1	12	5.2	0.27	2.191	0.173
<b>Reconstruction</b>							
C	9	8.1	12	3.7	0.37	2.191	0.123
	11	8.1	12	4.2	0.27	2.191	0.140
	13	8.1	12	4.7	0.27	2.191	0.157
	15	8.1	12	5.2	0.27	2.191	0.173
	8	11.1	12	3.7	0.37	2.191	0.123
	10	11.1	12	4.2	0.37	2.191	0.140
	12	11.1	12	4.7	0.37	2.191	0.157
	14	11.1	12	5.2	0.37	2.191	0.173
<b>Reconstruction</b>							

## 2.2 Damage assessment

Damage in physical scale models of rubble-mound breakwaters was here characterized by three methods: counting the number of displaced units, measuring the eroded area and measuring the damage depth of the profile. In the last case, Broderick (1983) and Van der Meer (1988) defined a dimensionless damage parameter,  $S = Ae/D_{n50}^2$ , where  $Ae$  is the eroded cross-section area around the still water level (SWL) and  $D_{n50}$  is the nominal diameter of the armour units (Figure 5). Melby and Kobayashi (1998) defined the local damage depth,  $e = (z_{before} - z_{after}) \cos \alpha$ , where  $z_{before}$  and  $z_{after}$  are the structure elevation before and after a test run, respectively, and  $\alpha$  is the structure slope (erosion of the profile being positive).



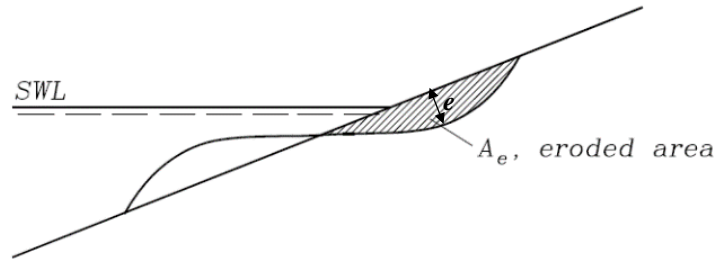


**Figure 5. Eroded area ( $A_e$ ) and eroded depth ( $e$ ) (adapted from U.S. Army Corps of Engineers, 2006).**

Different measuring techniques can be used for these damage assessment methods, such as, visual observation or stereo-photogrammetry. These techniques have the main advantage that they do not require emptying the flume before measurements are taken.

However, visual observation can only be applied to identify the unit displacements and movements, and it is very dependent on the technician experience. On the other hand, stereo-photogrammetry can be applied to both damage progression methods since the counting method can be achieved by photo analysis and the eroded area can be determined through comparison of cross-section profiles. Note that its efficiency depends on the characteristics of the environment (light, color of the bloc units, etc.). Moreover, stereo-photogrammetry can give much more information than the visual observation.

The software package used allows a complete 3D reconstruction environment, using stereo-image pairs as input. It consists of two distinct applications implemented in MATLAB™ (Ferreira et al., 2006) each with a specific objective:

- Camera calibration, which consists of identifying the parameters describing the projective cameras and their position and orientation within the observed world;
- Scene reconstruction, which consists of identifying depth from two different views of the same scene.

The output of the package consists of a (x, y, z) file describing the cloud of surveyed points. This is a standard file format which can be imported by various modelling tools. Using a MATLAB™ algorithm (Lemos and Santos, 2013), it is possible to create regular grids, enabling to extract the breakwater surveyed surface, as well as profile definition, in order to quantify the eroded area ( $A_e$ ) and, subsequently, the non-dimensional damage parameter ( $S$ ).

Since the used scene-reconstruction software rectifies the distortion introduced by the air-water interface, it is possible to reconstruct both the emerged and the submerged scenes thus avoiding the requirement of emptying the tank.

### 3 RESULTS AND DISCUSSION

#### 3.1 Counting displaced armour units

The number of displaced armour units was determined both visually and by analyzing the photos obtained with a camera placed above the model. Figure 6 to Figure 8 show an overview of the cross-section before the tests and after the last test for storm sequences A, B and C, respectively.

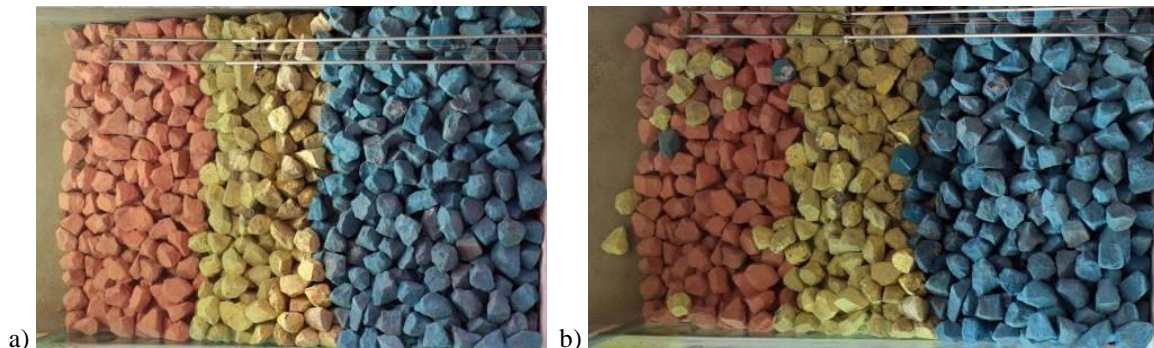


**Figure 6. Storm sequence A: a) cross-section before Test 1; b) cross-section at the end of Test 7.**

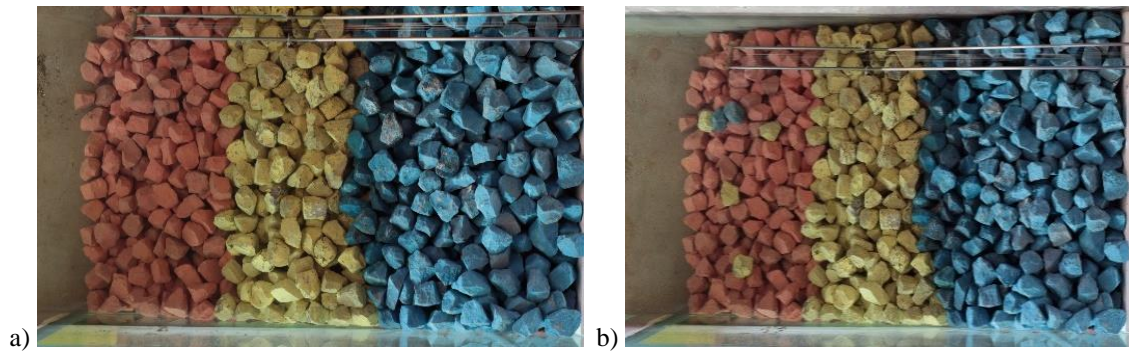


Figure 7. Storm sequence B: a) cross-section before Test 8; b) cross-section at the end of Test 15.

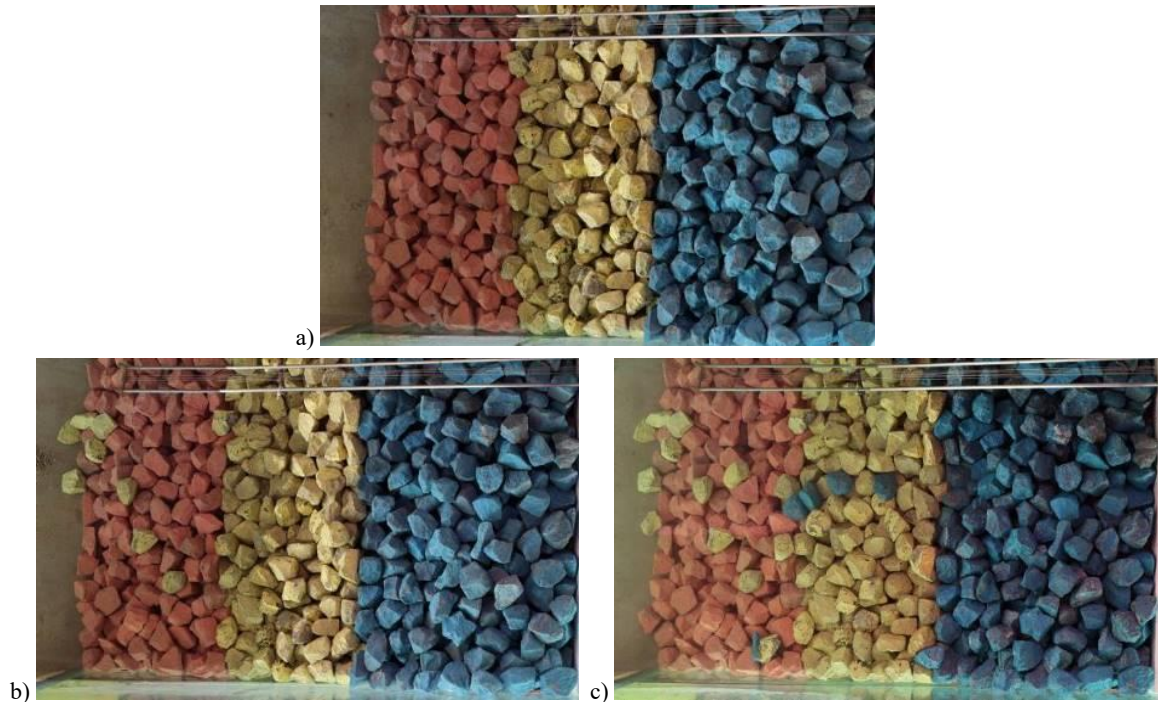


Figure 8. Storm sequence C: a) cross-section before Test 9; b) cross-section at the end of Test 15; c) cross-section at the end of Test 14.

As can be seen, in storm sequence C, after Test 15 (all with low water level), only yellow blocks were displaced, since the active zone was inside the yellow blocks zone. After Test 14, i.e., after the tests with high water level, blocks from a wider active zone (including blue and yellow blocks) had been displaced from their original positions, as in the case of storm sequences A and B.

Table 2 and **Error! Reference source not found.** show the damage occurred in each test for storm sequences A, B and C in terms of percentage of displaced blocks over the total number of blocks on the active zone,  $D$ .

Table 2. Percentage of displaced armour units ( $D$ ) for each storm sequence

Storm A	Test	1	2	3	4	5	6	7	
	$D$ (%)	3.2	4.0	4.8	5.6	7.3	9.7	10.5	
Storm B	Test	8	9	10	11	12	13	14	15
	$D$ (%)	4.0	4.8	6.5	6.5	7.3	8.9	10.5	11.3
Storm C	Test	9	11	13	15	8	10	12	14
	$D$ (%)	3.2	3.2	4.0	9.7	11.3	14.5	14.5	16.1

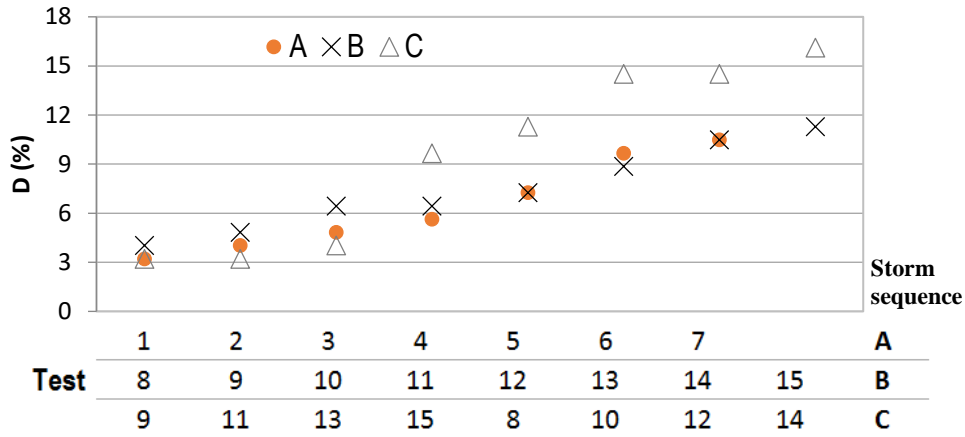


Figure 9. Storm sequences A, B and C. Damage in terms of percentage of displaced armour units ( $D$ ).

According to the damage classification referred to in the Coastal Engineering Manual (U.S. Army Corps of Engineers, 2006), the cumulative damage at the end of the last test of each sequence corresponds to an intermediate damage (units are displaced but without causing exposure of the under or filter layers to direct wave attack). However, some differences between sequences were found in the damage.

The highest percentage of displaced armour units in the first three tests occurred for storm sequence B and the difference increases from test to test. For these tests, storm sequences A and C were run with low water levels, whereas for storm sequence B, the water level changed from test to test, showing the influence of the water level in the armour damage.

After the fourth test, the trend changed, with storm sequence C presenting the highest damage. For the fourth test, the main difference between storm sequences is the value of the significant wave height, with storm sequence C having a value of  $H_s$  1.5 m and 1.0 m higher than the values tested for storm sequences A and B, respectively. After that test, the cumulative damage continues growing in the three sequences, with similar values of parameter  $D$  for sequences A and B, despite the differences in the wave conditions.

### 3.2 Calculation of damage parameter ( $S$ ) and eroded depth ( $e$ )

Data obtained during the tests with the photogrammetry were analyzed in order to calculate the damage parameter and the eroded depth. During the three test series, a survey of the undamaged profile was carried out ( $T_0$ ), followed by a survey at the end of each test run, in order to compare the eroded area between consecutive surveys. For a better damage characterization, the armour layer was divided into five profiles, 10 cm apart (Figure 10).

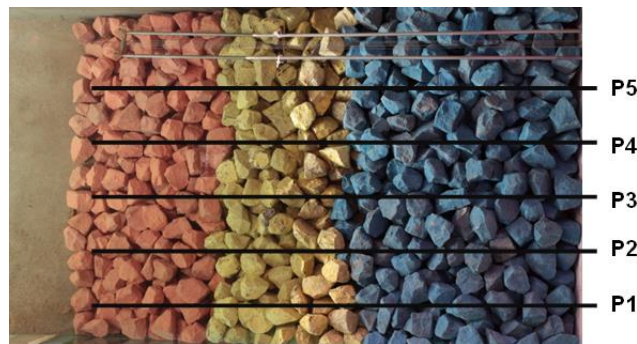


Figure 10. Location of surveyed profiles.

To obtain the eroded area for all the profiles, a MATLAB™ code (Lemos and Santos, 2013) was used, having as input the point clouds resulting from the reconstruction files. It enables the extraction of the pre-defined profiles for all the surveys, including the initial survey (undamaged profile,  $T_0$ ). The second step of the code compares all the profiles with their initial surveys and measures the corresponding eroded areas. Finally, the last step of the code consists in the calculation of the damage parameter ( $S$ ) and the eroded depth ( $e$ ). The main advantage of this methodology is that it is possible to choose the number and the position of the profiles to be analyzed even after finishing the survey.

Figure 11 illustrates the damage parameter  $S$  for profiles P1 to P5 for storm sequences A, B and C. Due to problems related with photo acquisition, results from test T1 for storm sequence A and T13 for storm sequence B are not presented. The most relevant eroded area occurred around the SWL, i.e., between 0.35 m and 0.7 m measured from the toe of the structure. Table 3 summarizes the non-dimensional damage parameter ( $S$ ) obtained for each profile at the end of the last test of the sequence.

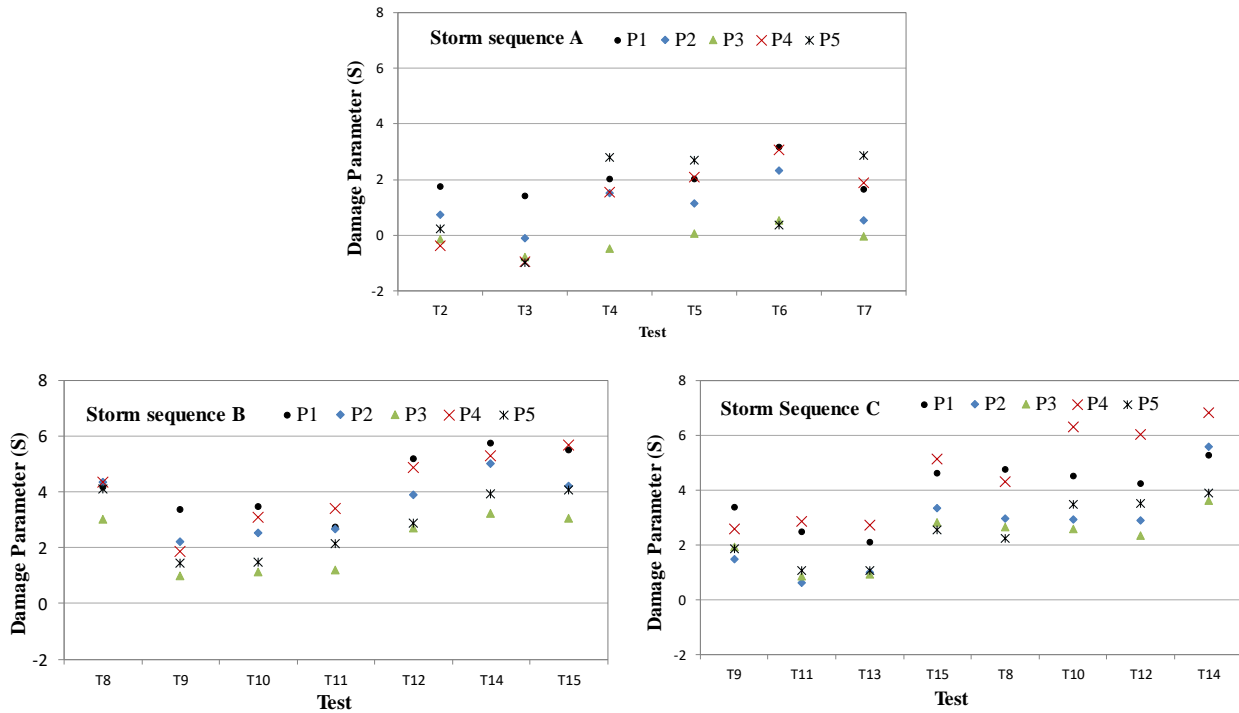


Figure 11. Storm sequences A, B and C. Damage parameter ( $S$ ) for Profiles P1 to P5.

Table 3. Damage parameter ( $S$ ) obtained at the end of storm sequences A, B and C

Storm sequences	$S$					
	Profiles					Average
	P1	P2	P3	P4	P5	
A	1.7	0.5	0.0	1.9	2.8	1.4
B	5.5	4.2	3.1	5.7	4.1	4.5
C	5.3	5.6	3.6	6.8	3.9	5.0

The analysis of **Error! Reference source not found.** and Table 3 shows clearly the influence of the water level variation in the  $S$  response. Tests with low water levels in sequences A (Tests 1 to 3), B and C (Tests 9, 11, 13, 15) correspond to lower values of  $S$  (**Error! Reference source not found.**, Table 1), when compared to the correspondent tests with high water level.

Comparing the different storm sequences, sequence A is the one with lowest values of  $S$  in all profiles. Sequences B and C exhibits similar mean  $S$  values. However, comparing the values for each profile, profiles P2 and P4 show some differences, with storm sequence C presenting the highest  $S$  values. As for the analysis of percentage of displaced armour units, sequence C seems to lead to higher damage than sequences A and B.

The average of the damage parameter ( $S$ ) for the five profiles at the end of storm sequences A, B and C, according to the damage classification proposed by Van de Meer (1988) for a 1:2 rock slope (Table 4), corresponds to initial damage for sequence A and to intermediate damage for sequences B and C.

Table 4. Damage level by  $S$  for a two-layer rock armour (Van der Meer, 1988)

Slope	Initial damage	Intermediate damage	Failure
1:1.5	2	3-5	8
1:2	2	4-6	8



There are significant differences on the cumulative damage at the different profiles, with profile P4 being the one where  $S$  is the highest for sequences B ( $S=5.7$ ) and C ( $S=6.8$ ), and with profile P5 being the profile where  $S$  is the highest one for sequence A ( $S=2.8$ ). In fact, the highest damage seems to have occurred for profile P4 (storm sequence C), reaching a value between intermediate damage and failure (Table 4).

On the other hand, only storm sequence A shows a negative erosion (accretion) in some profiles, especially for profiles P3 and P4. This occurred mainly for tests with low water level and corresponds to either rocks that moved between profiles or were both deposited and removed.

Based on the surveys for all profiles, the cumulative value of  $e/D_{n50}$  was calculated. The cumulative value of  $e/D_{n50}$  is the value of the erosion depth,  $e$ , measured at the end of the last test of each sequence, divided by the nominal diameter of the armour rock for which 50% of the total rock mass is smaller,  $D_{n50}$  (Hofland et al., 2011, 2017).

Figure 12 shows the surveys for profile P4 during storm sequence B, together with the variation of  $e/D_{n50}$  with the cross-shore coordinate ( $x$ ) along the slope cross-section, with  $x$  origin at the toe of the structure. Figure 13 presents the variation of  $e/D_{n50}$  calculated for the last test of each sequence A, B and C. As referred before, results for Test 13 for storm sequence B are not presented.

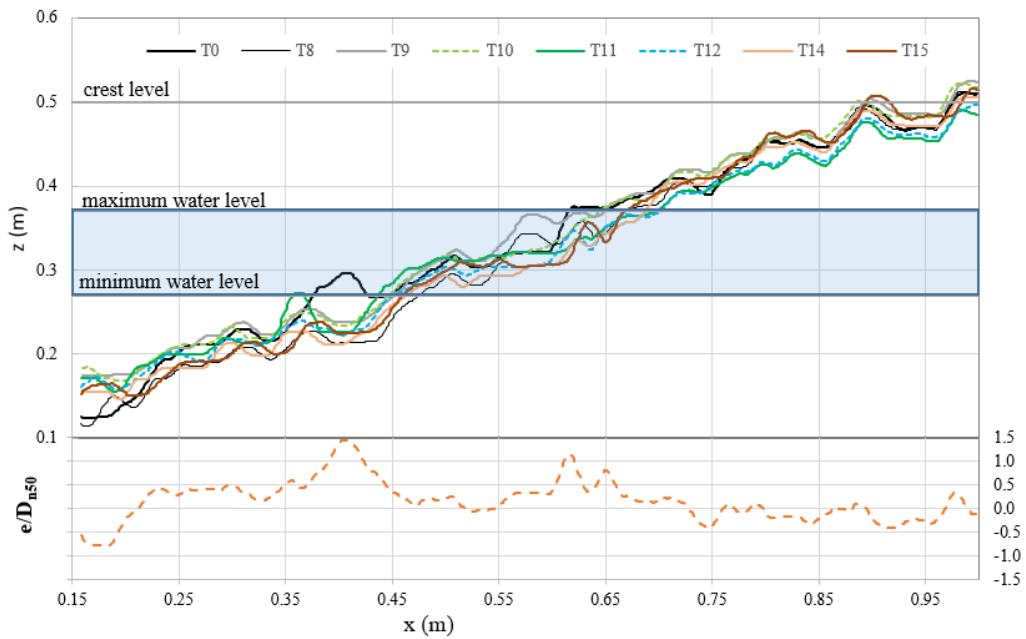


Figure 12. Profile P4 for each test of storm sequence B and  $e/D_{n50}$  between T0 and T15

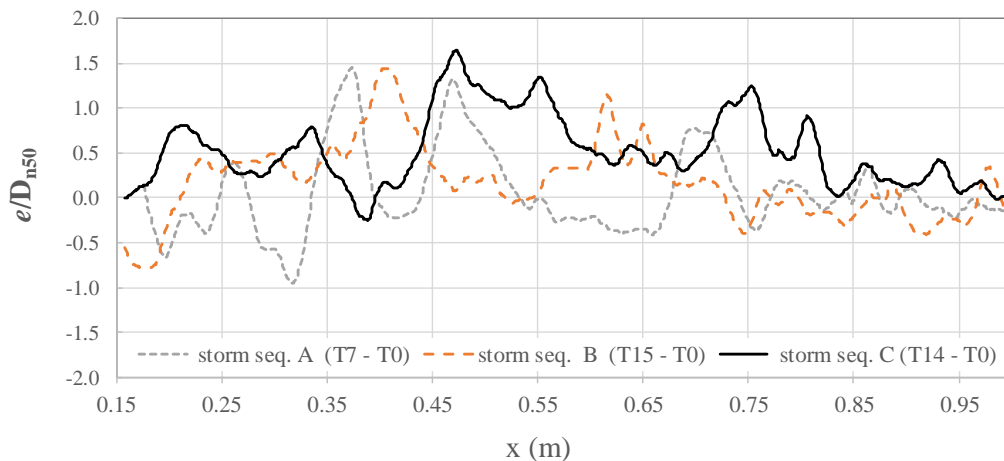


Figure 13. Profile P4.  $e/D_{n50}$  between T0 and the last test of storm sequences A, B and C.

For profile P4, and for storm sequence B, it can be observed that the damage is higher for  $x$  between 0.35 m and 0.65 m, i.e., on the active zone. As expected, within the active zone, for the same water level, the size of the hole increases with the wave height. It can also be observed that the hole size increases with the water level.

Comparing storm sequences, storm sequence C is the only one that presents cumulative values of  $e/D_{n50}$  higher than 1.5 and with more  $x$  extension, with values higher than 1. For this profile, the position where the hole is larger than one stone diameter,  $e > D_{n50}$ , changes with the storm sequence. Storm sequence A, where water levels tested are lower, presents the lowest values of  $x$  ( $0.35 < x \text{ (m)} < 0.48$ ) for  $e > D_{n50}$ . On the other hand, storm sequence C presents the highest values

of  $x$  for  $e > D_{n50}$  ( $0.45 < x \text{ (m)} < 0.76$ ). For all test series, damage is located in a region with  $x$  ranging between 0.35 m and 0.76 m.

#### 4 CONCLUSIONS

This paper describes the physical model tests of a rock-armour breakwater performed in a wave flume at LNEC, to characterize the damage evolution under future climate change scenarios. The tests were done by using two different damage evaluation techniques: visual observation and stereo-photogrammetric techniques. The percentage of displaced armour units,  $D$ , and the damage parameter,  $S$ , were calculated, together with the dimensionless local damage depth,  $e/D_{n50}$ . Five profiles were considered for the characterization of damages.

Cumulative test series with three different storm sequences were simulated: approach A, simulating increasing wave heights with increasing peak periods and water levels; approach B, corresponding to a storm sequence with a constant wave period and alternating water levels; and approach C, simulating, for two water levels, a standard storm build-up, with a constant peak period.

For approach B, due to the fact that the water level alternates between low and high water levels, the damage exhibited an oscillating behaviour, with two main damage areas corresponding to the active zone of each level. This behaviour differs significantly from the common storm sequences usually tested, where the water level does not change, and reproduced in storm sequences A and C.

Storm sequence C, which simulates a standard storm build-up, with a constant peak period for both water levels, showed the highest cumulative percentage of displaced armour units and the highest mean value of the damage parameter  $S$ , even though with similar values to storm sequence B. Analysing the dimensionless damage depth, storm sequence C was also the one that presented higher cumulative values.

In the present work, only five profiles were considered for averaging the damage, which may lead to some errors in the evaluation of the eroded area. Therefore, in the future, the eroded volume will be measured and divided by the length of the cross-section, Pedro et al. (2015).

#### ACKNOWLEDGEMENTS

This work was carried out under the framework of H2020 project HYDRALAB+ Adaptation for Climate Change, EC contract no 654110.

#### REFERENCES

- Broderick, L.L. (1983). Riprap stability, a progress report. Proc. Coastal Structures '83, American Society of Civil Engineers, pp. 320–330.
- Ferreira, R., Costeira, J.P., Silvestre, C., Sousa, I. and Santos, J.A. (2006). Using stereo image reconstruction to survey scale models of rubble-mound structures. Proc. CoastLab 2006, Porto, Portugal, pp. 107-116.
- Hofland, B., Santos, P., Taveira-Pinto, F., Almeida, E., Mendonça, A., Lemos, R. and Fortes, C.J.E.M. (2017). Measuring damage in physical model tests of rubble mounds. Proc. Coasts, Marine Structures and Breakwaters 2017, 5 - 7 September, Liverpool Waterfront, UK.
- Hofland, B., Van Gent, M.R.A., Raaijmakers, T. and Liefhebber, F. (2011). Damage evaluation using the damage depth. Proc. Coastal Structures 2011, Yokohama, Japan.
- HYDRALAB+ (2017). Deliverable: Task 8.1 Critical review of challenges for representing climate change in physical models. Report of HYDRALAB+ project - EC contract no 654110.
- Lemos, R. and Santos, J.A. (2013). Photogrammetric profile survey in scale model tests of rubble-mound breakwaters. Proc. SCACR 2013 – International Short Course/Conference on Applied Coastal Research, 4 - 7 June, Lisbon, Portugal.
- Lemos, R., Santos, J.A. and Fortes, C.J.E.M. (2017). Rubble mound breakwater damage assessment through stereo photogrammetry in physical scale laboratory tests. Ribagua - Revista Iberoamericana del Agua, 15p. ISSN: 2529-8968. <http://dx.doi.org/10.1080/23863781.2017.1381455>. <http://www.tandfonline.com/doi/full/10.1080/23863781.2017.1381455>
- Melby, J.A. and Kobayashi, N. (1998). Progression and variability of damage on rubble mound breakwaters. Journal of Waterway, Port, Coastal, and Ocean Engineering, 124(6), pp. 286–294.
- Pedro, F., Bastos, M., Lemos, R., Fortes, C.J.E.M. and Santos, J.A. (2015). Toe berm damage progression analysis using a stereophotogrammetric survey technique. Proc. SCACR 2015 – International Short Course/Conference on Applied Coastal Research, 28 Sept - 1 Oct, Florence, Italy.
- Troch, P. (2005). User Manual: Active Wave Absorption System. Gent University, Department of Civil Engineering, December.
- U.S. Army Corps of Engineers (2006). Coastal Engineering Manual. Engineer Manual 1110 2 1100, U.S. Army Corps of Engineers, Washington, D.C. (6 volumes).
- Van der Meer, J.W. (1988). Rock Slopes and Gravel Beaches under Wave Attack. Ph.D. thesis, Delft University of Technology, The Netherlands; also Delft Hydraulics Publ. 396.